Experimental Study on the Development Characteristics and Controlling Factors of Microscopic Organic Matter Pore and Fracture System in Shale

Qin Zhang [1,2]*, Zaiyang Liu [3], Chang Liu [4], Xiaomin Zhu [1,2], Ronald J. Steel [5], Hanyun Tian [1], Kai Wang [1] and Zeping Song [1]

[1]College of Geosciences, China University of Petroleum (Beijing), Beijing, China, [2]State Key Laboratory of Petroleum Resources and Prospecting, China University of Petroleum (Beijing), Beijing, China, [3]CNPC Chuanqing Drilling Engineering Company Limited Downhole Service Company, Chengdu, China, [4]CNOOC Research Institute Ltd., Beijing, China, [5]Department of Geological Sciences, University of Texas at Austin, Austin, TX, United States

Research on microscopic pore and fracture system of shale is a hot spot in the field of unconventional petroleum geology. Micro- and nano-scale organic matter pores in shale play a vital role in the accumulation of hydrocarbons. Research on the types, evolution rules and controlling factors of organic matter pore-fracture system in shale reservoirs can provide scientific guidance for the prediction of shale "sweet spots". In this paper, taking the shales from the Napo Formation, Oriente Basin, the Shahejie Formation, Zhanhua Sag, Bohai Bay Basin, and the Longmaxi and Wufeng Formations, Sichuan Basin as an example, the developmental characteristics of organic matter pore-fracture system were systematically studied using thin section, argon ion profiling scanning electron microscopy, X-ray diffraction, N_2 adsorption and desorption, geochemistry experiments, and image processing technology. The types of shale organic matter pores were divided into kerogen-hosted pores, organic matter microfractures (intra-organic matter and organic matter edge microfractures), and asphalt pores (or intra-asphalt pores). The circumferences of organic pore were generally within 100 nm, and the areas of most pores were smaller than 1,000 nm^2. Face rates of the organic pores were generally less than 1.5%, and the proportion of shale samples with a shape factor of 1 reached more than 50%. In addition, the deviation angles of organic matter pores at (0°, 45°) reached 90%, which showed that most of the organic matter pores tended to be oriented pores. The increase in the degree of thermal evolution provided driving force for the formation of circular pores in the organic matter. Internal factors (abundance of organic matter, kerogen types, and maturity) and external factors (diagenesis and mineral composition) controled the development of shale organic matter pores. Maturity, TOC content and inorganic minerals such as clay and pyrite content were positively correlated with the development of organic matter pores. However, brittle minerals caused a decrease in the face ratio of organic matter pores. Diagenetic compaction caused the

organic matter pores being deformed or eventually disappeared. This research can provide scientific guidance for the high-efficiency exploration of hydrocarbons in shale.

INTRODUCTION

With the successful development of the North American shale gas industry, research on the microscopic pore structures in shale has become an emerging hot topic (Curtis, 2002; Zou et al., 2010; Zou et al., 2011; Dong et al., 2012; Santosh and Feng., 2020). According to the previous studies, unconventional gas shale has special reservoir structures and hydrocarbon accumulation mechanism (Zhang et al., 2004; Dong et al., 2009). The microscopic pore structures of shale affected its hydrocarbon storage capacities significantly (Zou et al., 2011; Ko et al., 2016; Sun et al., 2016; Nie et al., 2018). Nano-scale pores and microfractures were well developed in organic-rich shales. Since microfractures were mainly developed in organic matter, therefore, the evolution of microfractures was affected by the evolution of organic matter significantly (Ko et al., 2016; Sun et al., 2016). The developmental characteristics of organic pores in shales with different sedimentary systems, maturities and depths were quite different (Chalmers and Bustin, 2007; Curtis et al., 2012). At present, the quantitative characterization methods of pores in porous media mainly include image analysis, fluid injection, nuclear magnetic resonance (NMR) and three-dimensional CT scanning methods (Wang et al., 2020). Nano-scale pores in shales can be observed through image analysis (SEM, TEM, etc.) (Reed et al., 2007; Zou et al., 2011). However, the image analysis method can only be used to observe the features of pores on the surface of the sample. On the contrary, fluid injection (MIP, nitrogen and carbon dioxide adsorption etc.), NMR, and nano-CT methods have effectively overcame this deficiency. Different fluid injection measurements can be applied to satisfy requirements of different pore size (Chen et al., 2013; Yang et al., 2013; Gai et al., 2016; Zhao et al., 2020). NMR and nano-CT tests can be used to characterize the morphology, connectivity, pore size, and distribution of pores in shale reservoirs (Chen et al., 2012; Curtis et al., 2012; Li et al., 2012; Chen, 2014; Tian et al., 2016).

The previous have proposed some classification standards for shale micro-pores (Loucks et al., 2009; Slatt and O'Brien, 2011; Yu, 2013). For example, according to the scheme proposed by Loucks et al. (2009), shale pores were classified into three categories: Intergranular, intragranular, and organic matter pores. However, there was no more detailed classification scheme for the types of organic pores. For organic-rich shales, organic pores play a vital role in the total pore space of shale (Jarvie et al., 2007; Chalmers et al., 2009; Curtis et al., 2012; Wang et al., 2018). Organic matter coexisted with inorganic minerals, and they can influence each other (Zhang et al., 1996). For example, montmorillonite has strong adsorption and ion exchange ability, it can be transformed into a clay-organic matter complex with a strong catalytic ability in the hydrocarbon generation process (Gao et al., 1990; Liu, 1995).

In addition, high organic matter contents, high maturity, and high-quality kerogen types all can promote the development of organic pores (Chen et al., 2016).

In this paper, taking the typical organic-rich shales in the Bohai Bay Basin, the Oriente Basin and the Sichuan Basin as an example, the developmental characteristics of organic matter pore-fracture system were systematically studied using thin section, argon ion profiling scanning electron microscopy, X-ray diffraction, N_2 adsorption and desorption, geochemistry experiments and image processing technology. This research can provide scientific guidance for the extraction of reservoir parameters, gas-bearing indicators and the rational deployment of exploration and development plans of shale reservoirs.

SAMPLES AND METHODS

Materials

In this study, 21 groups of shale samples were collected from three regions and three layers, namely the Napo Formation, Oriente Basin, Ecuador, the Shahejie Formation, Zhanhua Sag, Bohai Bay Basin, and the Longmaxi and Wufeng Formations, Sichuan Basin (**Figure 1**). These three types of shale samples were collected from different regions and different depositional environments. However, all these shale samples have good hydrocarbon generation conditions. Among them, the Napo Formation shales are stable shallow sea shelf deposits with high organic matter content and dominated by Type II kerogen (R_o is greater than 0.5%); the Shahejie Formation shales are shallow lake-semi-deep lake deposits with large shale thickness and high organic matter abundance; the Longmaxi and Wufeng Formations are deeper shallow shelf facies deposits, with high organic matter abundance, large shale rock thickness and high maturity. The differences in sedimentary environment will cause differences in the composition, type and abundance of organic matter within the rock. Moreover, the thermal evolution degrees of shales in different regions are quite different, which may be the controlling factors that cause the differences in the development of organic matter pore systems.

Experiments

1) Petrology, geochemistry and isothermal N_2 adsorption experiments.

A Quanta 200F field emission environmental scanning electron microscope was used to observe the microscopic pore structures of the shale samples. The samples were cut into blocks of 1.5 cm × 1 cm × 3 mm and subjected to argon ion polishing treatment. The image information of the organic pores on the shale surface was obtained by scanning electron microscope
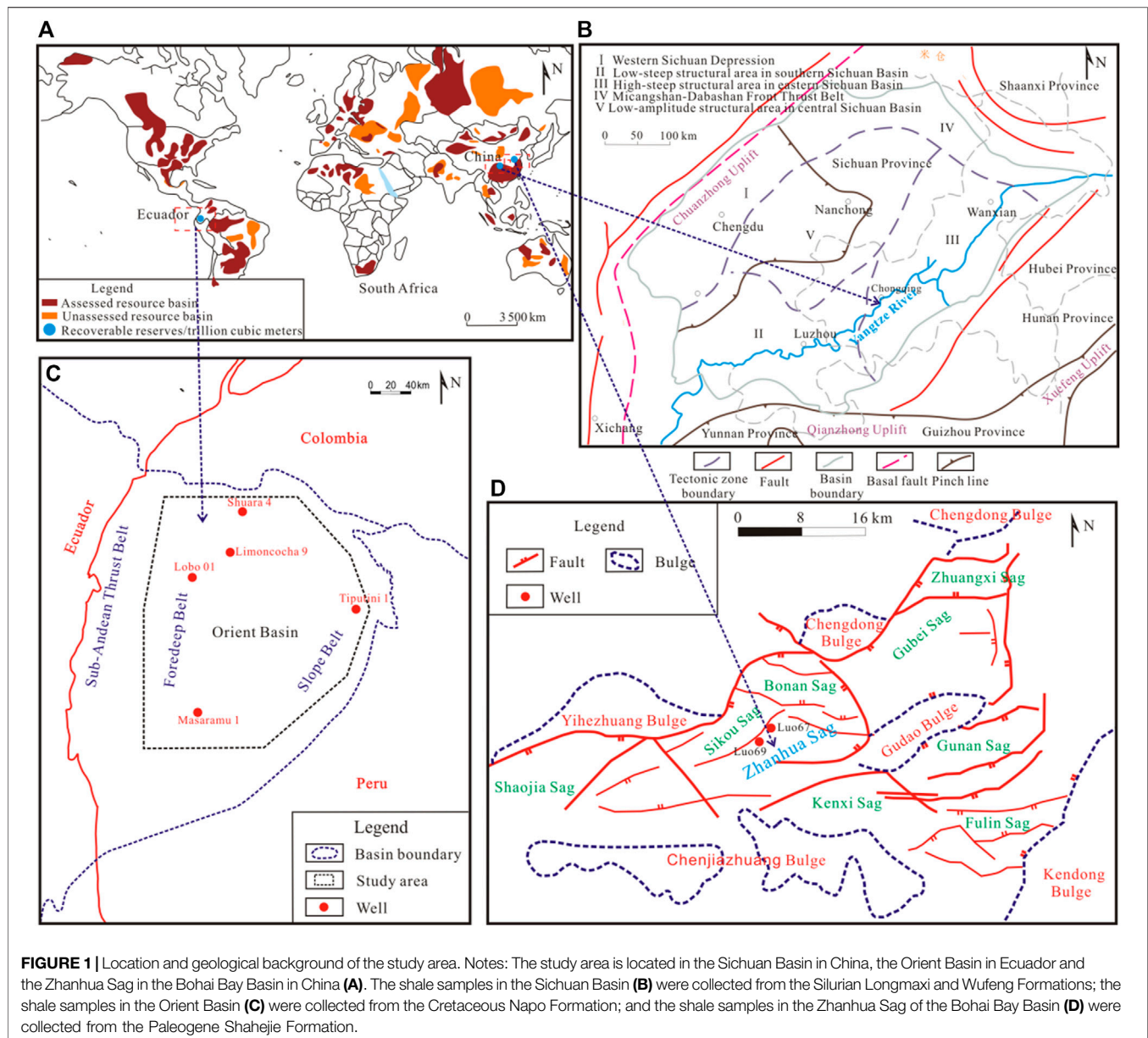
FIGURE 1 | Location and geological background of the study area. Notes: The study area is located in the Sichuan Basin in China, the Orient Basin in Ecuador and the Zhanhua Sag in the Bohai Bay Basin in China **(A)**. The shale samples in the Sichuan Basin **(B)** were collected from the Silurian Longmaxi and Wufeng Formations; the shale samples in the Orient Basin **(C)** were collected from the Cretaceous Napo Formation; and the shale samples in the Zhanhua Sag of the Bohai Bay Basin **(D)** were collected from the Paleogene Shahejie Formation.

observations. Moreover, the composition of minerals were determined through energy spectrum analysis.

The mineral composition detections of shale samples were realized via a D8 ADVANCE X-ray diffractometer; and the XRD experiments were used to obtain the content of main minerals and clay minerals in the samples. In addition, a CS230 analyzer was used to obtain the organic carbon content of shale after removing inorganic carbon. Geochemical parameters such as pyrolysis peak temperature T_{max} and hydrogen index HI were obtained using a Rock-Eval 6 Standard pyrolysis apparatus. The maturity of organic matter was obtained by the extraction of kerogen from shale combined with a vitrinite reflectance measuring instrument.

The isothermal N_2 adsorption experiments used a Quantachrome®Autosorb- iQ2-MP instrument from China University of Petroleum (Beijing). This instrument was used to

measure the volume, specific surface area, and diameter of shale pores. BET (Brunauer Emmett Teller) equation was used to calculated the pore surface area, while the pore volume and pore size distribution were obtained using the Barrett, Johner and Halenda (BJH) methods.

2) Image processing technology.

In this paper, ImageJ Processing Software was used to perform pore segmentation on SEM images after argon ion polishing. The software can perform threshold segmentation of organic matter pores, and the pore structure parameters such as the area shape coefficient and face ratio of the organic pores in the field of view can be obtained. Among them, the Feret diameter is the distance between the two furthest points of the organic pores. The two-

FIGURE 2 | Classification of pore shape factors (After Yao and Zhao, 2010, modified).
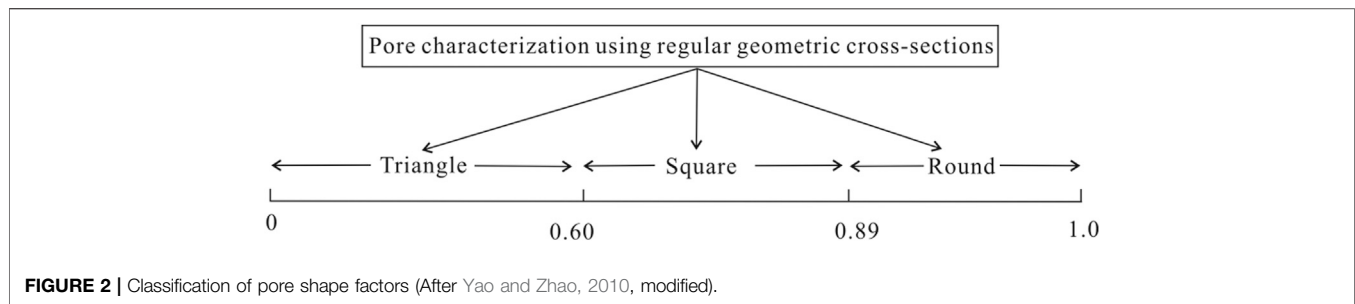
TABLE 1 | Composition and content of minerals in shale samples in the study area.

No.	Serial number	Depth (m)	Mineral composition (%)								Relative content of clay minerals (%)				
			Total clay	Quartz	Potash feldspar	Plagioclase	Calcite	Siderite	Dolomite	Pyrite	K	C	I	I/S	Interlayer ratio (%S)
1	L67	3,244.3	27	17	—	1	46	—	4	5	5	4	24	67	15
2	L67	3,270.6	23	15	—	1	53	—	3	5	3	3	30	64	15
3	L67	3,274.3	35	18	—	1	31	—	6	9	—	—	23	77	15
4	L67	3,275.8	22	14	—	—	56	—	4	4	—	—	32	68	20
5	L67	3,299.6	13	9	—	—	73	—	2	3	—	—	34	66	20
6	L67	3,307.4	13	8	—	—	73	—	4	2	—	—	43	57	15
7	L67	3,310.2	7	9	—	1	78	—	4	1	—	—	49	51	15
8	L67	3,317.2	27	17	—	—	39	—	11	6	10	4	22	64	15
9	L67	3,347.4	21	13	—	—	53	—	10	3	8	3	22	67	15
10	XYS9	3,378.8	33	24	—	2	29	—	6	6	—	/	25	75	15
11	XYS9	3,379.9	33	29	—	2	23	—	5	8	—	/	26	74	15
12	XYS9	3,416.0	26	16	—	—	47	—	6	5	—	/	28	72	15
13	MAI-2	4,090.4	79.9	16.4	1.7	—	—	—	—	2	45	-	11	44	10
14	SH4-1	2,738.0	61.3	2.6	—	—	—	36.1	—	—	44	16	10	30	5
15	L01-1	2,951.3	69.9	28	2.1	—	—	—	—	—	63	14	8	15	10
16	L9-3	2,884.0	66.9	27.8	2.4	—	—	—	—	2.9	49	12	7	32	10
17	Tp1-1	1,586.2	62.7	37.3	—	—	—	—	—	—	77	15	4	4	10
18	La-1	2,480.0	11.6	62.1	—	2.2	8.8	—	13.4	1.9	7	6	88	—	—
19	Lb-1	2,483.0	15.9	69.7	—	2.3	4.6	—	5.6	1.8	6	6	88	—	—
20	Lc-1	2,477.0	46.3	36.5	—	3.9	4.4	—	5	3.9	/	/	90	10	35
21	WF-1	2,570.0	15.7	51.8	—	2.1	15.7	—	12.3	2.4	5	6	89	—	—

Notes: No. 1–12 samples were collected from the Shahejie Formation; No. 13–17 samples were collected from the Napo Formation; No. 18–20 samples were collected from the Longmaxi Formation; and No. 21 sample was collected from the Wufeng Formation; K-Kaolinite; C-Chlorite; I-Illite; I/S- Imon mixed layers.

dimensional morphological features of pores were used to describe the roughness of organic pores, which was defined as:

$$ff = 4 \cdot \pi \cdot S/C^2 \qquad (1)$$

Where ff is the shape factor, S is the pore area, and C is the pore circumference (Jiao, 2015).

The cross-sectional shapes of different regular aggregates represent pores (**Figure 2**) (Yao and Zhao, 2010). At present, it is difficult to accurately extract the proportion of pores on organic matter. Thus, the percentage of organic matter pore area to the total area under the same view field was used to characterize the pore content.

In addition, the measured 135° circular organic matter pore angle was used as a statistical baseline. The difference between measuring angle of Feret diameter and 135° was used to describe the directional properties of organic pores, which was defined as:

$$G = |F - 135°| \qquad (2)$$

Where G is the deviation angle and F is the measurement angle of Feret's diameter.

EXPERIMENTAL RESULTS

Petrology and Geochemical Parameters

The results of whole rock and clay content XRD experiments were shown in **Table 1**. Experiments showed that the black shale of the Shahejie Formation was dominated by clay minerals and calcareous minerals; among them, the content of calcareous minerals ranged from 28 to 82%; while the content of clay minerals was only 7–35%; the content of the Imon mixed layers in clay minerals was between 51 and 77%. The Napo Formation samples were mainly composed of clay minerals and quartz; the content of clay minerals was high,

FIGURE 3 | Mineral composition and content of the shale samples. Notes: "Napo"- Napo Formation shales in Orient Basin; "S"- Shahejie Formation shales in Bohai Bay Basin; "L + W"- Longmaxi and Wufeng Formation shales in Sichuan Basin.
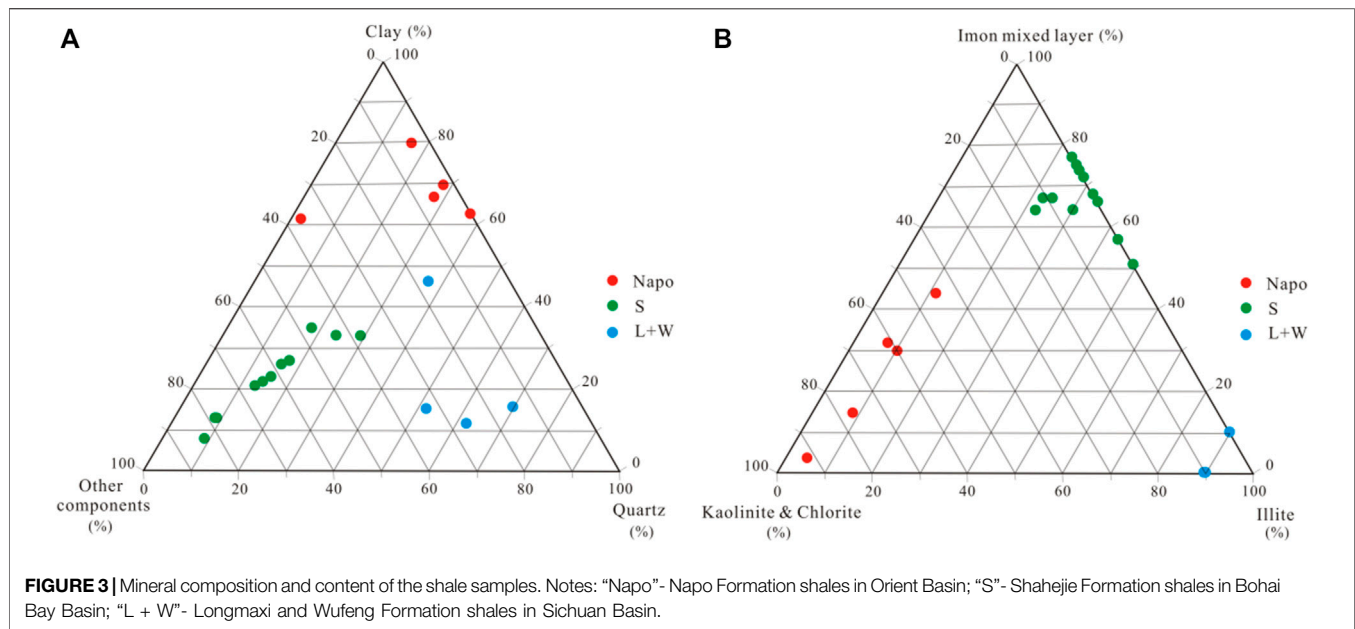
TABLE 2 | Experimental results of geochemical parameters of the shale samples in the study area.

Basin	Formation	Serial number	Depth (m)	TOC (%)	R_o (%)	HI	T_{max} (°C)	Organic matter type	Pore structure parameters (N₂ adsorption)		
									Specific surface area (m²/g)	Pore volume (cc/g)	Pore diameter (nm)
Bohai Bay Basin	Shahejie Formation	Y117-1	3,386.5	0.65	0.542	236.20	446	II₁	12.45	0.016	1.432
		L67	3,313.6	4.80	0.551	107.50	443	II₂	0.621	0.005	29.396
		BS5-1	4,764.5	1.50	1.731	18.67	577	II₁	6.106	0.007	1.432
		Y120	3,570.5	1.95	0.585	439.49	441	II₁	0.537	0.003	12.554
		Y117-2	3,347.0	4.44	0.524	720.72	440	I	0.401	0.001	4.887
		BS5-2	5,454.7	1.47	3.314	1.36	502	I	1.589	0.005	4.887
Orient Basin	Napo Formation	MA1-2	4,090.4	2.08	0.754	95.00	452	II₂	0.667	0.002	5.199
		SH4-1	2,738.0	1.79	0.922	90.00	445	II₂	0.461	0.001	5.199
		L01-1	2,951.3	2.12	1.087	153.00	447	II₂	0.627	0.001	1.688
		L9-3	2,884.0	1.69	0.755	231.00	447	II₁	0.167	0.001	3.169
		TP1-1	1,586.2	2.15	0.646	140.00	447	II₂	4.660	0.011	3.969
Sichuan Basin	Longmaxi Formation	La-1	2,480.0	3.99	3.08	0.08	600	I	15.007	0.015	3.607
		Lb-1	2,483.0	3.68	3.10	0.07	600	I	15.813	0.016	1.688
		Lc-1	2,477.0	3.41	3.02	0.06	600	I	18.085	0.019	3.794
		Ld-1	2,455.0	3.46	2.51	/	/	/	15.259	0.011	1.432
	Wufeng Formation	WF-1	2,455.0	3.73	3.26	0.05	600	I	15.240	0.016	3.794

Notes: HI- Hydrogen index, HI = S_2/TOC; T_{max}- Peak temperature.

ranging from 61.3 to 79.9%. The Longmaxi and Wufeng Formation shale samples contained extremely high quartz content, ranging from 36.5 to 69.7%; while the content of clay minerals was relatively low; the content of illite accounted for about 88–90% of the total clay minerals. The content of the main minerals (**Figure 3A**) and clay minerals (**Figure 3B**) of the shale samples in the three regions has a certain difference.

Shale samples from 15 wells in three study areas were selected to determine the abundance, type and maturity of organic matter. The results are shown in **Table 2**. The TOC content of the Napo Formation samples ranged from 1.69 to 2.15%; Type II kerogen

(mainly Type II₂) was developed; R_o ranged from 0.646 to 1.087% (mature stage). The TOC content of the Shahejie Formation samples ranged from 0.65 to 4.8%; Type I and II kerogen (II₁ and II₂) were developed; R_o ranged from 0.524 to 3.314%. The Longmaxi and Wufeng Formation samples have a high TOC content ranging from 3.41 to 3.99%; Type I kerogen was developed; R_o ranged from 3.08 to 3.26%. On the whole, the Longmaxi and Wufeng Formation shales have the strongest hydrocarbon—generating ability, followed by the Shahejie Formation, while the hydrocarbon—generating ability of the Napo Formation is relatively poor.

FIGURE 4 | Distribution characteristics of pore structure parameters of shale samples. Notes: **(A)** Pore diameter distribution; **(B)** Pore circumference distribution; **(C)** Pore area distribution; **(D)** Face rate distribution; **(E)** Shape factor distribution; **(F)** Deviation angle distribution.
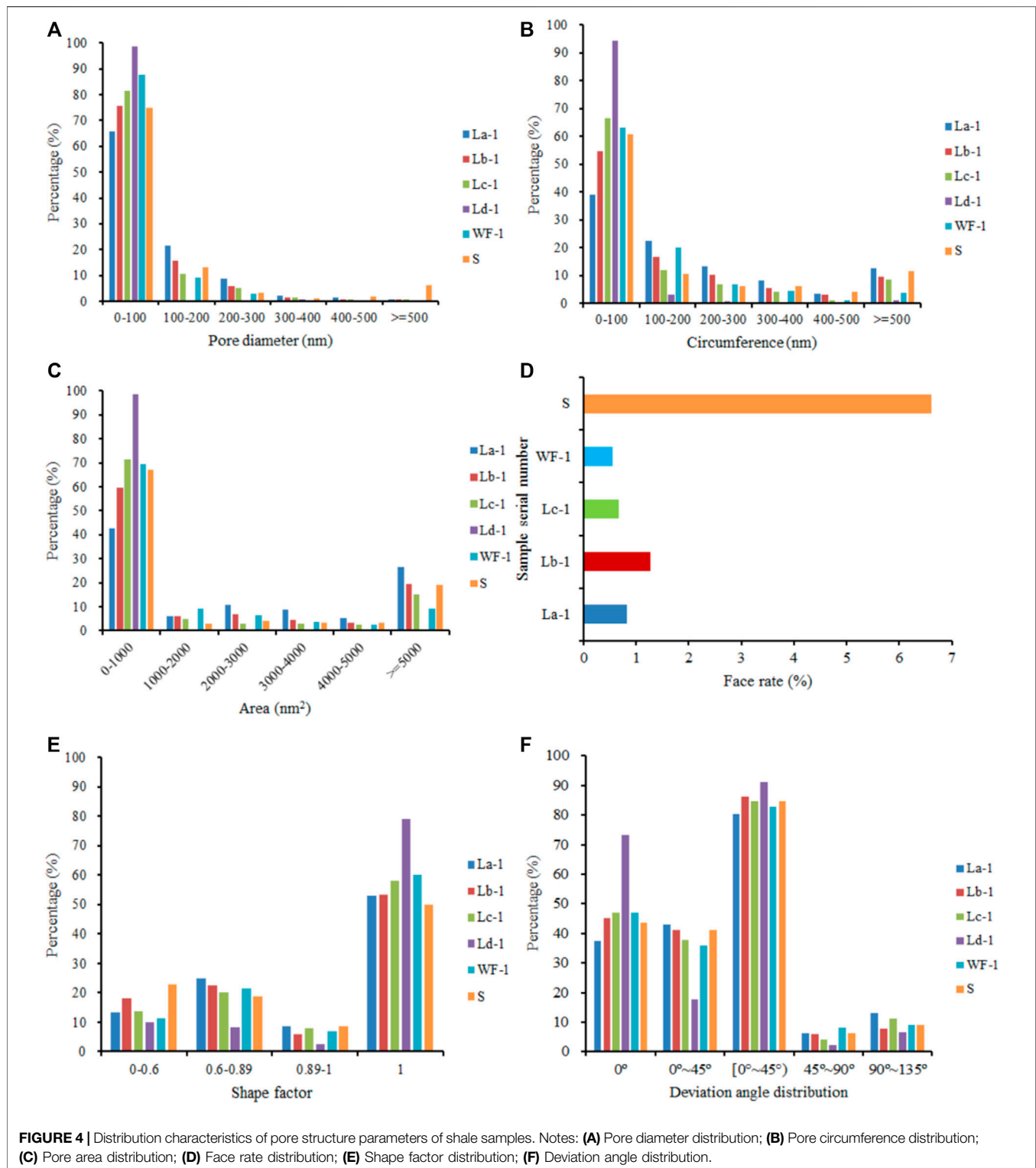
Pore Structure Parameters

Studies have shown that the higher the thermal evolution degree of organic matter, the more developed the organic matter pores (Milliken et al., 2013). Therefore, shale samples with different thermal evolution degrees were selected for comparative research on the development characteristics of organic pores, which can help us better understand the evolution mode of organic pores (Milliken et al., 2013).

Data statistics and analysis of 29 representative images in 6 wells showed that the organic pore diameter (**Figure 4A**) and

circumference (**Figure 4B**) of different shale samples generally within 100 nm. In this interval, the proportion of organic matter pores are all greater than 50%. Meanwhile, the statistical results of the pore area (**Figure 4C**) showed that the area of most pores was smaller than 1,000 nm^2, but there were also many pores with an area greater than 5,000 nm^2. The difference in pore diameter, circumference and area content of organic matter pores is obviously affected by the degree of thermal evolution (Cui et al., 2012).

The face rate of the organic matter pores in the argon ion polished scanning electron microscope images was calculated (**Figures 4D–F**). The results showed that the face rate of the Longmaxi and Wufeng Formation shales was relatively low, which was generally less than 1.5%. Except for the Lb-1 well, the shale samples of the other wells have a face rate of less than 1%. The shale samples from Well BS5 of Shahejie Formation have a significantly higher face rate than samples from the Longmaxi and Wufeng Formations. This may be due to the fact that the field of view is less, and there is a larger error (Loucks et al., 2009; Li et al., 2020).

The range of pore diameters of the shale samples measured by the nitrogen adsorption experiments is shown in **Table 2**. The pore diameters of the Napo shale samples ranged from 1.688 to 5.199 nm; the pore diameters of Longmaxi and Wufeng Formation (L, W) shales ranged from 1.432 to 3.794 nm, and their pore volume and specific surface area were larger than those of the other two regions; the pore diameters of the Shahejie Formation (S) shales ranged from 1.432 to 29.396 nm, and the pore diameter varies greatly.

The pore volume of all shale samples ranged from 0.001 to 0.019 cc/g. Among them, the samples of Longmaxi and Wufeng Formations have a larger average pore volume, ranging from 0.011 to 0.019 cc/g, while those of the Napo Formation have the smallest average pore volume, ranging from 0.001 to 0.011 cc/g. The test results of the specific surface area are similar to the pore volume. The samples of the Longmaxi and Wufeng Formations have the largest specific surface area, ranging from 15.24 to 18.085 m^2/g, while the samples of the Napo Formation have the smallest specific surface area, ranging from 0.167 to 4.66 m^2/g.

DISCUSSION

Developmental Characteristics of Organic Matter Pores

Observations under the microscope showed that organic pores have various shapes, including round, elliptical, triangular, slit-shaped, honeycomb, beaded, and irregular (**Figure 5**). The structural parameters of organic pores in shale can well characterize the development characteristics of pores. Moreover, the shape, connectivity, concentration and directional properties of pores all have a significant influence on the large-scale accumulation of shale gas and the formulation of development plans (Hao et al., 2006; Houben et al., 2013; Kuila et al., 2014; Wu et al., 2014; Wu et al., 2015; Jiao et al., 2017).

Micron and nano-scale organic pores are mostly round (shape factor 0.89–1), indicating that their initial shapes are usually round (**Figures 5A–E**). The larger the pores, the more complex their morphology. Observations showed that there were few circular pores for the larger pores, and the morphology of these pores tended to be elliptical or irregular (**Figures 5F–H**). As the maturity of shale increased, organic pores of various shapes were formed, which was also the main reason for the formation of irregular pores. In addition, the organic pores may merge together, and then became flower-like (**Figure 5E**) or irregular pores with good connectivity (**Figure 5B**). Some pores have even undergone severe deformation or collapse due to strong compaction (**Figure 5D**).

Organic matter pores have strong heterogeneity. The more pores develop inside the rock, the better its connectivity (**Figure 5D**). For low maturity shale, there were few organic pores, so the connectivity of pores and microfractures in the rock was poor. The spatial distribution of organic pores were classified into two categories: directional type and chaotic type. When the external pressure was high, the long axis direction of the organic pores was consistent with the extension direction affected by plastic deformation (**Figure 5E**).

The distribution of pores in the same piece of organic particles was usually similar (**Figure 5A**). However, there were also cases where even within the same organic matter, the size and development of pores were quite different (**Figure 5H**). This was because, as the thermal evolution continued, the small pores became larger and merged into large pores (**Figure 5H**). Then, the shape and development of pores became complex, and the heterogeneity of shale pore structures gradually became significant. In some microscopic views, large numbers of organic pores merged to form pore clusters, while in other microscopic views, isolated organic pores may be still the main ones. The symbiosis of organic matter and pyrite was easy to be observed in shale samples, and the pyrite intercrystalline pores and oval organic pores were mainly developed (**Figure 5I**). In the shale sample of Well Lc-1 (2,483 m), it was also found that some extremely small organic pores appeared on the boundary between organic matter and titanium dioxide (**Figure 5J**).

In addition to organic matter pores, organic matter microfractures were also very developed in shale samples. In this study, organic matter microfractures were further divided into intra-organic matter microfractures (**Figure 5K**) and organic matter edge microfractures (**Figures 5L,M**). Organic matter microfractures generally had a long strip or slit-shaped structure, and their formation was closely related to the diagenetic shrinkage of kerogen (**Figures 5N,O**).

The statistical results showed that the proportion of shale samples with a shape factor of 1 reached more than 50%. Moreover, the proportion of pores with a shape factor of 0.89–1.00 was close to 10%, that is, the pores in the samples were mainly round or close to round. This showed that during the thermal evolution process, the pore morphology tended to develop into circular pores. The proportion of pores that tended to be square (0.60–0.89) was between 8.32 and 37.57%. While the proportion of organic pores with a shape factor of 0–0.60 was between 9.86 and 22.75%, and its content was similar to that of pores that tended to be square (**Figure 4E**).
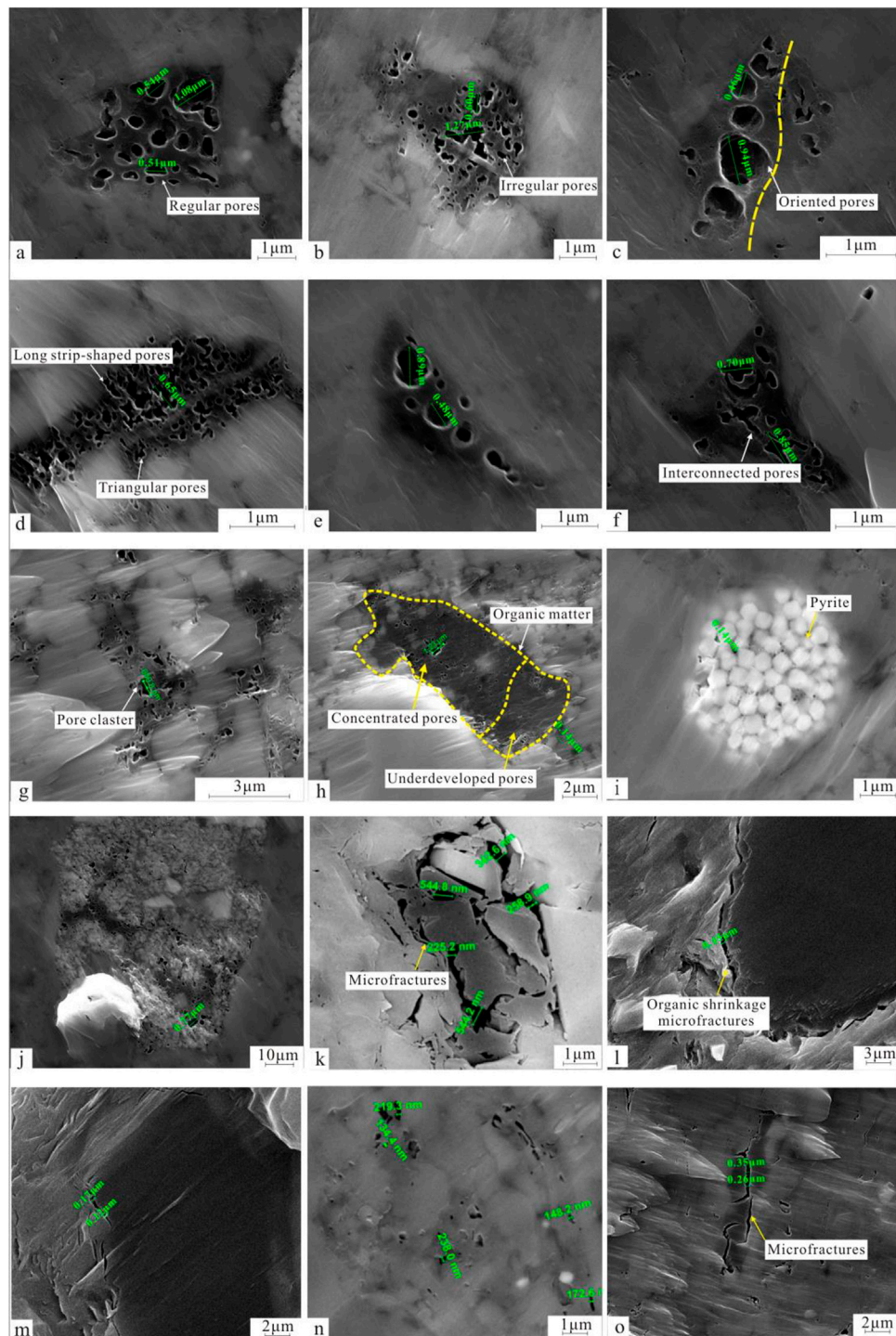
FIGURE 5 | Argon ion polishing scanning electron microscope images of shale samples from Oriente Basin, Bohai Bay Basin and Sichuan Basin. Notes: **(A)** Well Lc-1, 2,483 m, round and elliptical organic matter pores with good connectivity; **(B)** Well WF-1, 2,455 m, irregular and elliptical pores; **(C)** Well Lc-1, 2,483 m, organic pores distributed in a beaded shape, with good orientation; **(D)** Well Lb-1, 2,483 m, triangular and long strip-shaped organic pores, the pores are disorderly distributed; **(E)** Well Lc-1, 2,483 m, flower-like distribution of organic matter pores; **(F)** Well Lc-1, 2,483 m, interconnected organic matter pores; **(G)** Well Lb-1, 2,483 m, pore clusters randomly distributed along the organic matter; **(H)** Well La-1, 2,480 m, different pore development levels on the same piece of organic matter; **(I)** Well WF-1, 2,455 m, symbiotic organic matter and pyrite accompanied by oval organic matter pores; **(J)** Well Lc-1, 2,483 m, organic pores developed at the boundary between organic matter and titanium dioxide; **(K)** Well BS5, 4,761.55 m, organic matter microfractures; **(L)** Well Y120, 3,507.2 m, organic shrinkage microfractures developed at the edge of organic matter; **(M)** Well Y120, 3,507.2 m, organic shrinkage microfractures; **(N)** Well BS5, 4,764.45 m, intra-organic pores and dissolution pores; **(O)** Well Y115, 4,004.1 m, matrix microfractures.
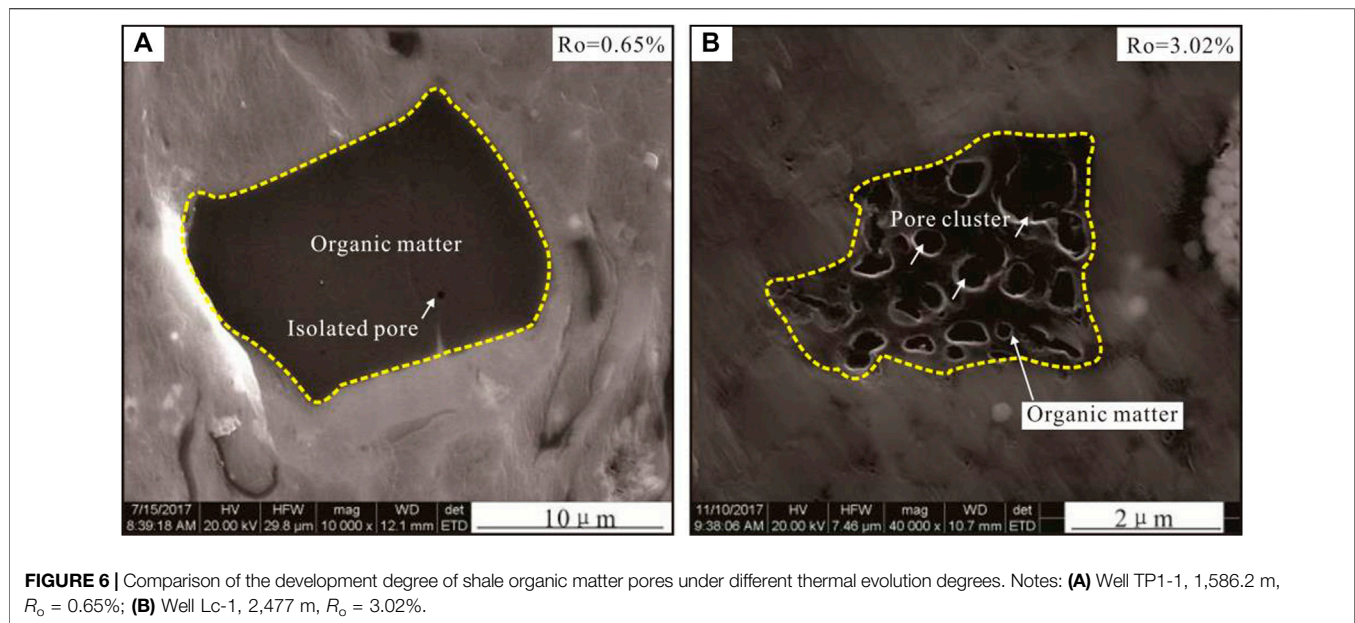
FIGURE 6 | Comparison of the development degree of shale organic matter pores under different thermal evolution degrees. Notes: **(A)** Well TP1-1, 1,586.2 m, R_o = 0.65%; **(B)** Well Lc-1, 2,477 m, R_o = 3.02%.

According to **Figure 6B**, for shale samples in the same area or in different areas, the deviation angle of the organic matter pores was mainly less than 45°. The proportion of shale samples with deviation angles less than 45° was absolutely dominant, with an average content of more than 80%. Oriented pores refer to pores that are round and had a deviation angle of 0°, and their proportion was generally greater than that of pores whose deviation angle was between 0° and 45°, but their proportions were relatively close (**Figure 4F**).

Statistics found that the deviation angle of organic matter pores in shale reservoirs at (0°, 45°) can reach 90% (**Figures 4E,F**). This showed that most of the organic matter pores tended to be oriented pores as a whole, and only part of the pores are randomly distributed. When the maturity of the organic matter was low, the organic matter pores were mainly small, round pores, and the degree of orientation was very good. However, as R_o continued to increase, the disordered distribution of organic pores gradually became significant. When the shale reached a large depth, the organic pores will undergo strong compaction and deformation, and the strong directional environmental stress may improve the directional properties of the pores. The increase of brittle minerals can increase the anti-compaction ability of organic pores, thereby weakening the directional properties of pores (Chalmers et al., 2009).

Classification of Organic Matter Pores

The previous have conducted preliminary studies on the microscopic pore classification in shale. For example, Zhang et al. (2016) divided shale pore system into pores and microfractures, while shale pores were further divided into matrix pores (intercrystalline pores and intragranular pores) and organic pores. However, there is no further fine division for the types of shale organic matter pores.

In this paper, organic pores in shale were divided into three major categories and four sub-categories combining research in

this paper and the classification schemes given by the previous (Jarvie et al., 2007; Loucks et al., 2009; Milliken et al., 2013; Yu., 2013; Lu et al., 2015; Zhang et al., 2016). The classification scheme in this study comprehensively considered the shapes, structures, location, origin and size of shale pores (**Table 3**).

According to **Table 3**, organic pores were divided into organic matter pores, organic matter microfractures and asphalt pores. Organic matter pores were kerogen-hosted pores. They have round, elliptical and irregular structures, and were mainly formed in the main hydrocarbon generation period. In addition, organic matter microfractures were divided into intra-organic matter microfractures and organic matter edge microfractures, both of which were related to organic matter shrinkage and are mainly formed in shales with low maturity. Moreover, the second cracking of asphalt for hydrocarbon generation can also form a large number of organic pores, and the shape, size and occurrence of the pores were similar to those of kerogen-hosted pores (**Table 3**).

Influence of Abundance and Maturity of Organic Matter on Development Degree of Organic Matter Pores

For the coupling relationship between organic pores and the maturity, it was found that the higher the shale maturity, the more organic pores develop. For example, in **Figure 6A**, the maturity of the shale sample from Well TP1-1 (1,586.2 m) is low, and its R_o is 0.65%. Observations under the microscope showed that the organic pores of the shale sample from Well TP1-1were not developed. In contrast, for the shale sample from Well Lc-1 (2,477 m) in **Figure 6B**, the R_o is 3.02%. Observations under the microscope showed that the organic pores were very developed.

The study also found that when the R_o of the shale samples was equivalent to immature and low-maturity conditions, there were

TABLE 3 | Classification of organic pore types in shale reservoirs.

Major category	Subcategory	Shape	Distribution and origin	Size	Occurrence
Organic matter pore	Kerogen-hosted pore	Round, oval, triangle, slit-shaped or irregular	Organic matter interior; Kerogen hydrocarbon generation	Nano and micro scale	Directional, messy
Organic matter microfracture	Intra-organic matter microfracture	Elongated or slit-shaped	Organic matter interior; Kerogen hydrocarbon generation	Nano and micro scale	Directional, messy
	Organic matter edge microfracture	Elongated or slit-shaped	Organic matter and mineral edges; Organic matter shrinkage	Nano and micro scale	Directional, messy
Asphalt pore	Intra-asphalt pore	Round, oval, triangle, slit-shaped or irregular	Asphalt interior; cracking and hydrocarbon generation of asphalt	Nano and micro scale	Directional, messy

FIGURE 7 | Changes in the morphology of organic matter pores under different thermal evolution degrees. Notes: **(A)** Well Y120, 3,507.2 m, $R_o = 0.59\%$, argon ion polishing image; **(B)** Well Y117, 3,401.93 m, $R_o = 0.56\%$, argon ion polishing image; **(C)** Well BS5, 4,764.45 m, $R_o = 1.73\%$, argon ion polishing image; **(D)** Well Lc-1, 2,477 m, $R_o = 3.02\%$, argon ion polishing image.
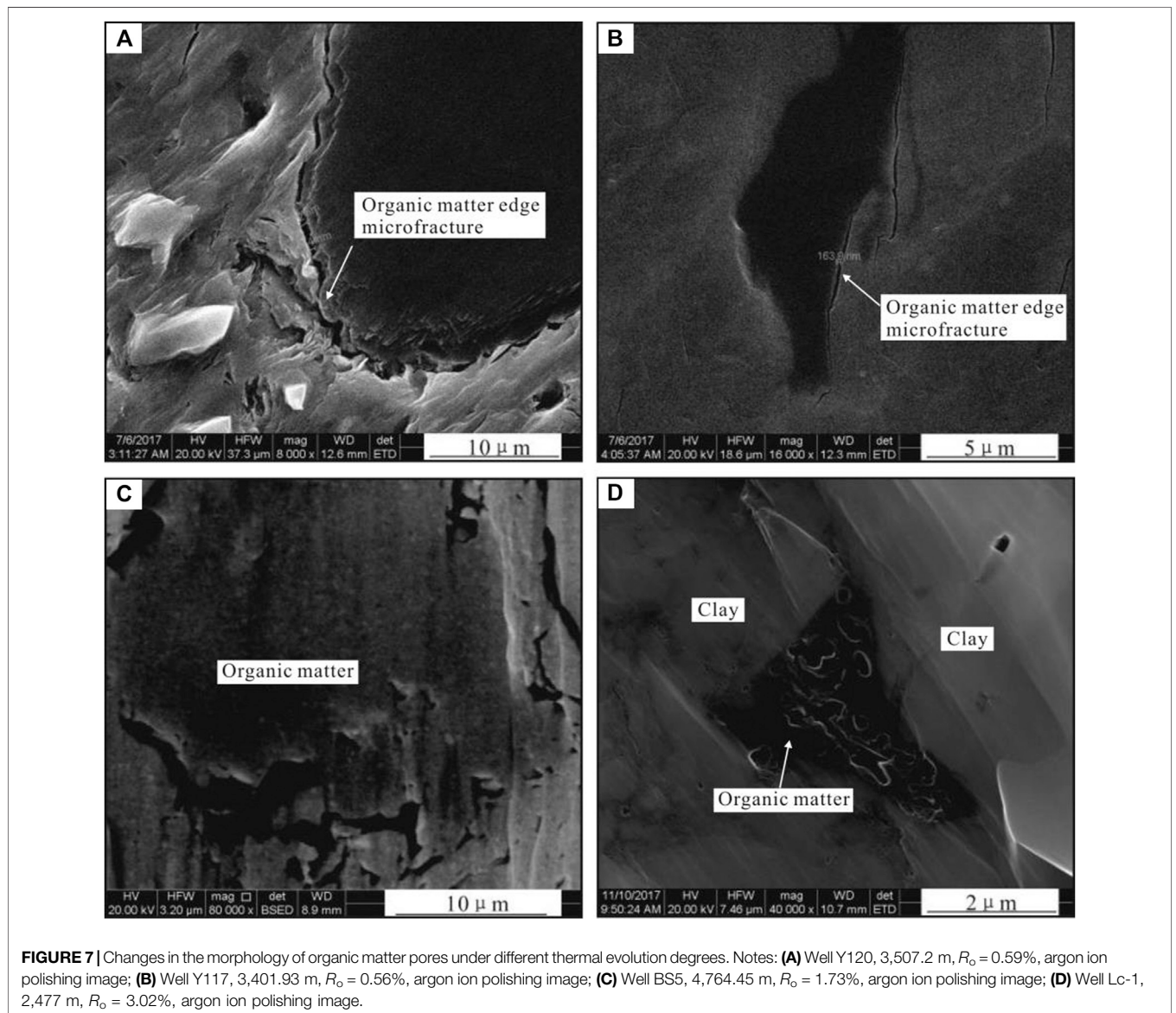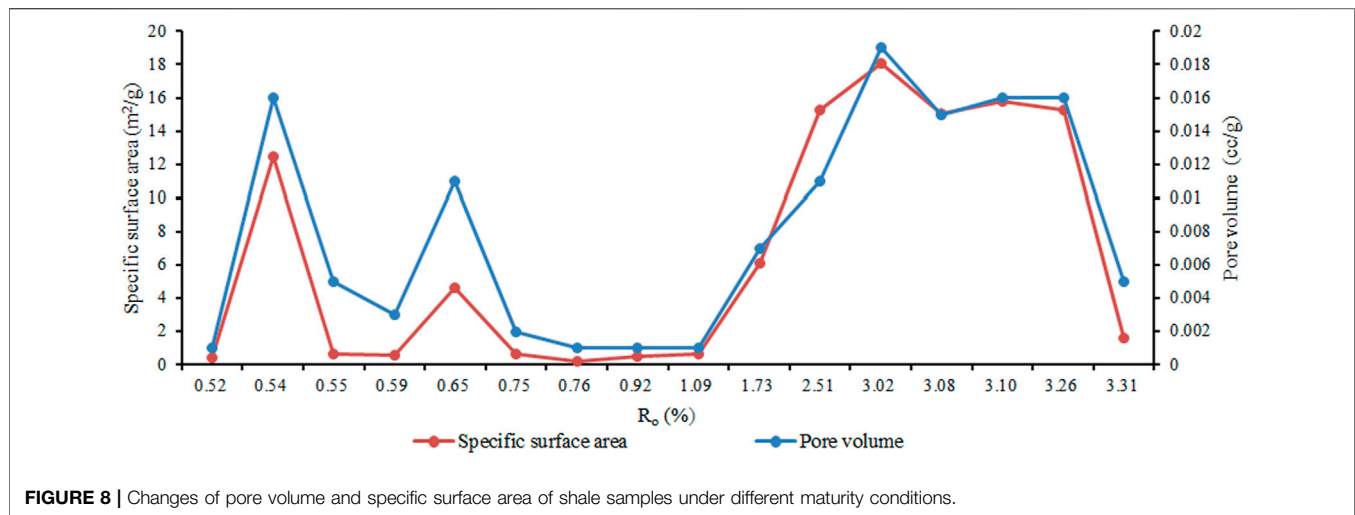
FIGURE 8 | Changes of pore volume and specific surface area of shale samples under different maturity conditions.

few organic pores in the shale, but large numbers of organic matter edge microfractures existed in the shale, such as the Well Y120 sample shown in **Figure 7A** (3,570.50 m, R_o = 0.59%) and the Well Y117 sample shown in **Figure 7B** (3,401.93 m, R_o = 0.56%).

Under mature and high-maturity conditions, strong hydrocarbon generation will promote the formation of a large number of organic matter shrinkage microfractures and intra-organic matter microfractures, such as the Well BS5 sample shown in **Figure 7C** (4,764.45 m, R_o = 1.73%).

When the shale reached the over-mature stage, almost all the pores are intra-organic matter pores, and almost all organic matter microfractures disappear. Meanwhile, organic matter edge microfractures can be transformed into organic pores, such as the Well Lc sample shown in **Figure 7D** (2,477.00 m, R_o = 3.02%).

The enrichment degree of organic pores are affected by many factors (Pommer and Milliken, 2015). These factors can be divided into two categories: internal factors (kerogen type, abundance, and maturity) and external factors (diagenesis and mineral composition). The study showed that as the shale maturity increased, the pore volume and specific surface area of the shale samples in the study area had the same changing trend (**Figure 8**). However, the pore structure parameters were in a fluctuating state as the shale maturity increased, that is, they didn't show a single upward or downward changing trend. In addition, the morphology of the correlation curves between pore diameter and cumulative pore volume can also be divided into three regions with significant differences (**Figure 9**). Therefore, the use of TOC or R_o alone cannot determine the changing trend of pore structure parameters well. This feature also reflected that the development characteristics of organic pores were not only controlled by a single factor (Li, 2021).

From **Figure 10**, it can be found that the relationship between TOC content and pore structure parameters of shale samples in different regions has a certain difference. The correlation of L-W sample data was very poor (**Figures 10A,B**), but when all

Longmaxi and Wufeng Formation samples were integrated, the data showed a good linear relationship (**Figures 10C,D**). For the samples from the Napo and Shahejie Formations dominated by inorganic pores, the correlation between specific surface area and pore volume and TOC was not obvious, and there were many abnormal points (**Figures 10A–D**). The abundance of organic matter provides a material basis for the evolution of organic matter pores. Generally, the higher the abundance of organic matter, the more abundant the organic matter pores. However, organic matter pores can develop in large quantities only when the organic matter reached mature stage. Therefore, the poor correlation showed that TOC content was not the only factor that affects the pore structures.

The types of kerogen mainly affect the development degree and morphology of organic matter pores. Many scholars have studied the differential evolution of shale organic matter pores (Bernard et al., 2012; Dong et al., 2015; Ma et al., 2017). The pore evolution process of different types of kerogen was different. For example, Dong et al. (2012) proposed that Type I kerogen was a "shrinkage type" and Type III kerogen was a "porous type", and partial sapropel kerogen was much more conducive to the development of organic pores. Jarvie et al. (2007) found that Type II kerogen was more prone to produce organic pores than Type I and III kerogens. Some scholars have found that when the chloroform bitumen "A" in shale was extracted, the pores increased significantly. Therefore, the retained oil will occupy the pore space generated by the hydrocarbon generation of organic matter. The kerogen in the Zhanhua Sag of the study area was dominated by Type I kerogen. During the rapid oil generation stage, as the degree of thermal evolution increased, the specific surface area and pore volume didn't show an increasing trend but decreased gradually (**Figure 7**). This may be due to the fact that the generated oil directly filled the pores. However, when R_o was high enough, different types of organic matter can generate a lot of pores, and then the kerogen type was no longer the main controlling factor of organic matter pores.

FIGURE 9 | Relationship between pore diameter and cumulative pore volume of shale samples in the study area.
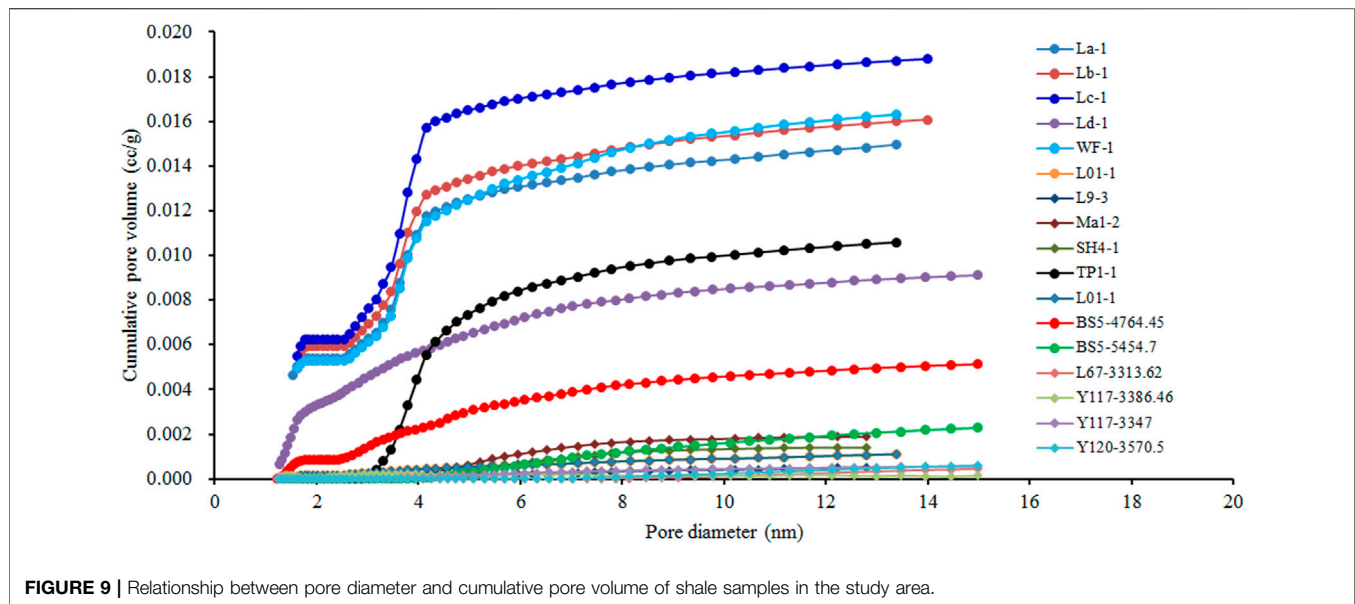
The correlation between R_o and pore structure parameters showed that the pore volume and specific surface area of Longmaxi and Wufeng Formation shales increased with the increase of R_o; however, this relationship was poor in Napo and Shahejie Formation shale samples (**Figures 10E,F**). Moreover, the pore volume and specific surface area of the Longmaxi and Wufeng Formations were much larger than those of the other two regions. The organic matter abundance and R_o of the Longmaxi and Wufeng Formation shale samples were high, and the R_o of the samples were all above 2%, which belong to the high-mature-over-mature shale. High-mature-over-mature shale mainly generated dry gas, and the escape of hydrocarbons will cause a significant increase in pore volume and specific surface area. The Napo and Shahejie Formation shale samples had a low degree of thermal evolution. In the immature-low maturity stage, the organic matter pores were relatively underdeveloped, and the organic matter shrinkage microfracture was an important pore type.

Some samples have higher R_o values. With the increase of R_o, the organic pores in shale develop from underdeveloped to highly developed, from small size to large size, from organic microfractures to organic pores, and from good orientation to disorderly development. Some correlations in **Figure 10** were poor, indicating that the influencing factors of the development of organic matter pores were complex, which were affected by the geological factors such as organic matter abundance, kerogen type, and different mineral composition.

Influence of Mineral Components and Diagenesis on Development Degree of Organic Matter Pores

Diagenesis and mineral composition also have a significant impact on the development of organic pores. Diagenesis has a

great impact on the preservation of organic matter pores. Strong compaction can cause the organic pores to be compressed, deformed, elongated, or even disappeared (Hao et al., 2006; Jiao et al., 2017; Wang et al., 2020). According to **Figure 11**, the pore volume and specific surface area values of the Longmaxi and Wufeng Formation samples were inversely proportional to the content of brittle minerals (**Figures 11A,B**), and directly proportional to the content of clay minerals (**Figures 11C,D**); however, these relationships were not significant for the Napo Formation shale samples.

A weaker hydrodynamic environment was conducive to the growth and reproduction of organisms, and thus the organic matter components will be relatively enriched. However, the content of clay minerals in this kind of sedimentary environment will be higher, and the content of brittle minerals dominated by terrigenous clastics will be less. Therefore, the increase in the content of brittle minerals reflected a gradually stronger hydrodynamic condition, which was not conducive to the evolution and preservation of kerogen. Meanwhile, the clay minerals coexisting with organic matter had a catalytic effect on the maturation of organic matter, which in turn facilitated the evolution of kerogen-hosted pores and will cause the specific surface area and pore volume being greatly improved. Therefore, the development of organic pores was positive to the content of clay minerals, and it was negative to the content of brittle minerals (**Figure 11**). It can also be seen from **Figure 11** that the correlation between the pore structure parameters and mineral components of the high maturity shales (Longmaxi and Wufeng Formation shales) was very good; however, the correlations between these parameters was poor in low-maturity shales (Napo Formation shales). This was because the Napo Formation shales have low maturity and
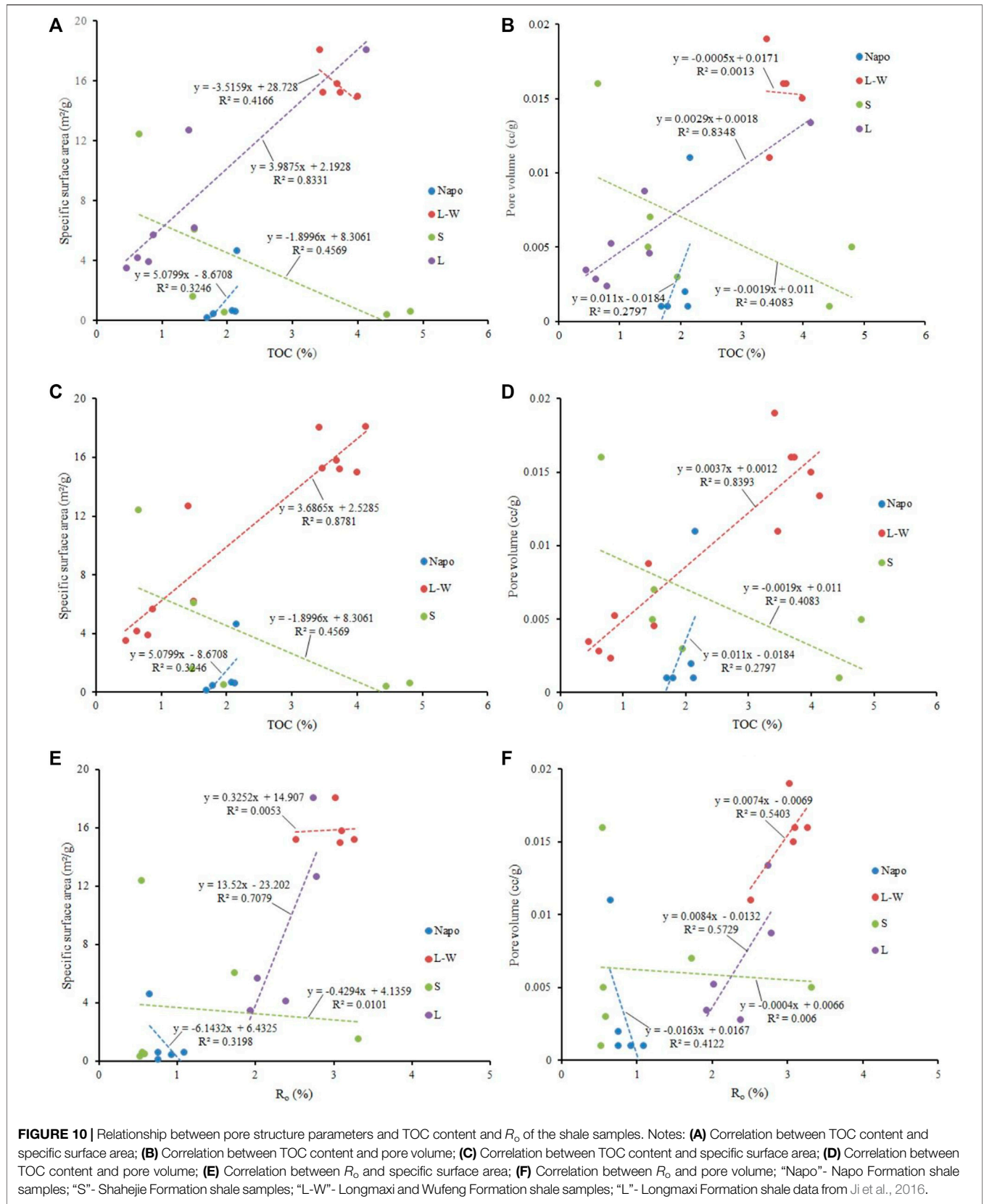
FIGURE 10 | Relationship between pore structure parameters and TOC content and R_o of the shale samples. Notes: **(A)** Correlation between TOC content and specific surface area; **(B)** Correlation between TOC content and pore volume; **(C)** Correlation between TOC content and specific surface area; **(D)** Correlation between TOC content and pore volume; **(E)** Correlation between R_o and specific surface area; **(F)** Correlation between R_o and pore volume; "Napo"- Napo Formation shale samples; "S"- Shahejie Formation shale samples; "L-W"- Longmaxi and Wufeng Formation shale samples; "L"- Longmaxi Formation shale data from Ji et al., 2016.

FIGURE 11 | Relationship between pore structure parameters and content of different mineral components of the shale samples. Notes: **(A)** Correlation between brittle mineral content and specific surface area; **(B)** Correlation between brittle mineral content and pore volume; **(C)** Correlation between clay mineral content and specific surface area; **(D)** Correlation between clay mineral content and pore volume; "Napo"- Napo Formation shales; "L-W"- Longmaxi and Wufeng Formation shales; "L"- Longmaxi Formation shale data from Ji et al., 2016.

underdeveloped organic pores, so the controlling factors of pore structure parameters were much more complicated.

Development Mode of Organic Matter Pores

In summary, the development of pores in shale reservoirs are affected by internal and external factors. Internal factors include organic matter abundance, kerogen type and maturity; and external factors include mineral components (brittle minerals, clay minerals and FeS) and diagenesis.

Organic carbon is the material basis of organic pores (Morozov et al., 2021). The higher the degree of thermal evolution of organic matter, the more developed the organic pores in shales (Wu et al., 2021). The kerogen type of organic matter is an important factor controlling the differential evolution of organic matter pores. Under the same or similar

TOC and R_o conditions, the specific surface area and pore volume of the microscopic pores of shales dominated by Type II kerogen were better than those of Type I kerogen, however, the organic pores in shale dominated by Type III kerogen were relatively underdeveloped (**Figure 12**). Organic matter maturity provides the driving force for the evolution of organic matter pores. Under the same TOC content, the higher the maturity, the more organic matter pores will develop.

However, under immature and low-maturity conditions, organic matter microfractures were developed in all types of kerogen. These microfractures were mainly organic-edge shrinkage microfractures, and organic pores were relatively underdeveloped (**Figures 7A,B**). With the increase of R_o, during the early-to-mid mid-diagenesis period, the microfractures developed at the edge of organic matter gradually transitioned into the interior of organic matter. However, in the mid-to-late mid-diagenesis period, the organic
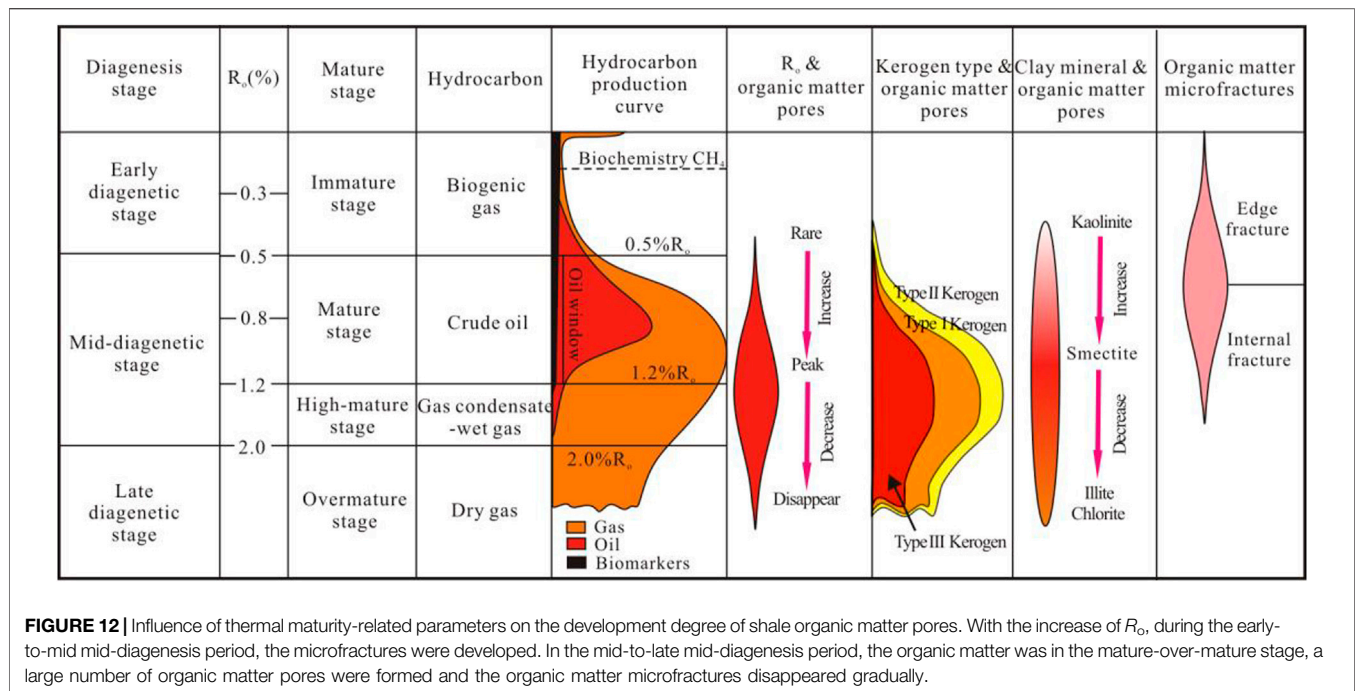
FIGURE 12 | Influence of thermal maturity-related parameters on the development degree of shale organic matter pores. With the increase of R_o, during the early-to-mid mid-diagenesis period, the microfractures were developed. In the mid-to-late mid-diagenesis period, the organic matter was in the mature-over-mature stage, a large number of organic matter pores were formed and the organic matter microfractures disappeared gradually.

matter was in the mature-over-mature stage, a large number of organic matter pores were formed and the organic matter microfractures no longer developed (**Figure 12**).

Diagenesis and different mineral compositions are external factors that affect the development of organic pores. Strong compaction can cause the organic pores deformed or even disappeared. Clay minerals and pyrite can promote the development of organic pores, while brittle minerals (such as quartz, feldspar and carbonate minerals) can inhibit the development of organic pores.

Overall, the development mode of organic pores in shale reservoirs is the coupling results of multiple geological factors (**Figure 12**). TOC and kerogen type are the most direct controlling factors. Under the premise of high degree of thermal degree, the higher the abundance of organic matter, the more organic pores developed; and under the same thermal degree, the development of organic pores satisfies: Type II kerogen > Type I kerogen > Type III kerogen. Thermal evolution or R_o is the source of organic matter pores. Only when the organic matter reaches the mature to high maturity range, the organic matter pores will develop in large numbers in the shales and have good connectivity.

CONCLUSION

1) In this paper, taking the typical shales from the Bohai Bay Basin, the Oriente Basin, and the Sichuan Basin as an example, argon ion profiling scanning electron microscopy, N_2 adsorption and desorption, geochemistry experiments and ImageJ software image processing technology were used to study the types and evolution of micro- and nano-scale organic matter pores in shale reservoirs.

2) The circumferences of organic pore were generally within 100 nm, and the areas of most pores were smaller than 1,000 nm^2. Face rates of the organic pores were generally less than 1.5%, and the proportion of shale samples with a shape factor of 1 reached more than 50%. In addition, the deviation angles of organic matter pores at (0°, 45°) can reach 90%, which showed that most of the organic matter pores tended to be oriented pores.

3) The organic pores of shale were divided into kerogen-hosted pores, organic matter microfractures (intra-organic matter and organic matter edge microfractures) and asphalt pores (intra-asphalt pores). As the degree of thermal evolution increased, the organic pores gradually tend to be round, and the directional properties of the pores was strengthened.

4) The development of shale organic pores was controlled by internal factors (abundance of organic matter, kerogen type and maturity) and external factors (diagenesis and mineral composition). Maturity promoted the development of organic pores; TOC content was positively correlated with the development of organic pores; and there were significant differences in the degree of development of organic pores in shale organic matter of different sedimentary conditions.

5) Clay minerals and pyrite can promote the development of organic pores, while brittle minerals can cause a decrease in the face ratio of organic pores. The diagenetic compaction will cause the organic pores to deform or eventually disappear. Finally, the development mode of shale organic matter pores was clarified combined with the development characteristics and influencing factors of organic matter pores.

6) Through this study, the development characteristics, evolution process and controlling factors of organic pores in shales formed in different sedimentary environments were compared. This research can provide scientific guidance for the extraction of evaluation parameters and gas-bearing indicators and the rational deployment of exploration and development plans of shale reservoirs.

DATA AVAILABILITY STATEMENT

The raw data supporting the conclusion of this article will be made available by the authors, without undue reservation.

AUTHOR CONTRIBUTIONS

QZ is responsible for the idea and writing of this article, and ZL, CL, XZ, RS, HT, KW, and ZS are responsible for the experimental part.

FUNDING

REFERENCES

Bernard, S., Wirth, R., Schreiber, A., Schulz, H.-M., and Horsfield, B. (2012). Formation of Nanoporous Pyrobitumen Residues during Maturation of the Barnett Shale (Fort Worth Basin). *Int. J. Coal Geology.* 103 (23), 3–11. doi:10.1016/j.coal.2012.04.010

Chalmers, G., Bustin, R. M., and Powers, I. (2009). *A Pore by Any Other Name Would Be as Small: The Importance of Meso-And Microporosity in Shale Gas Capacity.* Denver, Colorado: AAPG Annual Convention and Exhibition, 7–10.

Chalmers, G., and Bustin, R. M. (2007). The Organic Matter Distribution and Methane Capacity of the Lower Cretaceous Strata of Northeastern Britishcolumbia, canada. *Int. J. Coal Geology.* 70 (1-3), 223–239. doi:10.1016/j.coal.2006.05.001

Chen, Q. (2014). *Characterization of Shale Pore Structure Based on High-Resolution Imaging Technology,* Master's thesis. Southwest Petroleum University, 1–5. (in Chinese with English abstract).

Chen, Q., Zhang, J., Tang, X., Li, W., and Li, Z. (2016). Relationship between Pore Type and Pore Size of marine Shale: An Example from the Sinian-Cambrian Formation, Upper Yangtze Region, South China. *Int. J. Coal Geology.* 158, 13–28. doi:10.1016/j.coal.2016.03.001

Chen, S., Xia, X., and Qin, Y. (2013). Pore Structure Classification of Longmaxi Formation Shale Gas Reservoirs in Southern Sichuan Enriched Area. *J. China Coal Soc.* 38 (5), 760–765. (in Chinese with English abstract).

Chen, T., Tang, D., and Xu, H. (2012). Fine Description of Coal Reservoirs in Hancheng Demonstration Area Based on X-CT Technology. *Geol. J. Universities* 18 (3), 505–510. (in Chinese with English abstract).

Cui, J., Zou, C., Zhu, R., Bai, B., Wu, S., and Wang, T. (2012). New Advances in Shale Porosity Research. *Adv. Earth Sci.* 27 (12), 1319–1325. (in Chinese with English abstract).

Curtis, J. B. (2002). Fractured Shale-Gas Systems. *AAPG Bull.* 86 (11), 1921–1938. doi:10.1306/61eeddbe-173e-11d7-8645000102c1865d

Curtis, M. E., Cardott, B. J., Sondergeld, C. H., and Rai, C. S. (2012). Development of Organic Porosity in the Woodford Shale with Increasing thermal Maturity. *Int. J. Coal Geology.* 103, 26–31. doi:10.1016/j.coal.2012.08.004

Curtis, M. E., Sondergeld, C. H., Ambrose, R. J., and Rai, C. S. (2012). Microstructural Investigation of Gas Shales in Two and Three Dimensions Using Nanometer-Scale Resolution Imaging. *Bulletin* 96 (4), 665–677. doi:10.1306/08151110188

Dong, C., Ma, C., Luan, G., Lin, C., Zhang, X., and Ren, L. (2015). Pyrolysis Simulation Experiment and Diagenesis Evolution Pattern of Shale. *Acta Sedimentologica Sinica* 33 (5), 1053–1061. (in Chinese with English abstract).

Dong, D., Cheng, K., Wang, S., and Lv, Z. (2009). An Evaluation Method of Shale Gas Resource and its Application in the Sichuan basin. *Nat. Gas Industry* 29 (5), 33–39. (in Chinese with English abstract).

Dong, D., Zou, C., and Yang, H. (2012). Progress and Development Prospects of Shale Gas Exploration and Development in China. *Acta Petrolei Sinica* 33 (S1), 107–114. (in Chinese with English abstract).

Gai, S., Liu, H., He, S., Mo, S., Chen, S., Liu, R., et al. (2016). Shale Reservoir Characteristics and Exploration Potential in the Target: A Case Study in the Longmaxi Formation from the Southern Sichuan Basin of China. *J. Nat. Gas Sci. Eng.* 31, 86–97. doi:10.1016/j.jngse.2016.02.060

Gao, X., Zhang, W., and Zhang, H. (1990). Erratum. *Mar. Pet. Geology.* 7 (2), 201–205. (in Chinese with English abstract). doi:10.1016/0264-8172(90)90048-l

Hao, F., Zou, H., and Fang, Y. (2006). Thermal Evolution and Hydrocarbon Generation Mechanism of Organic Matter in Overpressure Environment. *Acta Petrolei Sinica* (5), 9–18. (in Chinese with English abstract).

Houben, M. E., Desbois, G., and Urai, J. L. (2013). Pore Morphology and Distribution in the Shaly Facies of Opalinus Clay (Mont Terri, Switzerland): Insights from Representative 2D BIB-SEM Investigations on Mm to Nm Scale. *Appl. Clay Sci.* 71, 82–97. doi:10.1016/j.clay.2012.11.006

Jarvie, D. M., Hill, R. J., Ruble, T. E., and Pollastro, R. M. (2007). Unconventional Shale-Gas Systems: The Mississippian Barnett Shale of north-central Texas as One Model for Thermogenic Shale-Gas Assessment. *Bulletin* 91 (4), 475–499. doi:10.1306/12190606068

Ji, W., Song, Y., and Jiang, Z. (2016). Micro-nano Pore Structure Characteristics and Controlling Factors of Longmaxi Formation Shale in southeastern Sichuan Basin. *Acta Petrolei Sinica* 37 (2), 182–195. (in Chinese with English abstract).

Jiao, K. (2015). *Genesis, Evolution Mechanism and Quantitative Characterization of Nanopores in Coal and Shale,* Master's thesis. Nanjing University, 1–7. (in Chinese with English abstract).

Jiao, K., Ye, Y., Liu, S., Ran, B., Deng, B., Li, Z., et al. (2017). Nanopore Characteristics of Super-deep Buried Mudstones in Sichuan Basin and its Geological Implication. *J. Chengdu Univ. Techn. (Natural Sci. Edition)* 44 (2), 129–138. (in Chinese with English abstract).

Ko, L. T., Loucks, R. G., Zhang, T., Ruppel, S. C., and Shao, D. (2016). Pore and Pore Network Evolution of Upper Cretaceous Boquillas (Eagle Ford-equivalent) Mudrocks: Results from Gold Tube Pyrolysis Experiments. *Bulletin* 100, 1693–1722. doi:10.1306/04151615092

Kuila, U., McCarty, D. K., Derkowski, A., Fischer, T. B., Topór, T., and Prasad, M. (2014). Nano-scale Texture and Porosity of Organic Matter and clay Minerals in Organic-Rich Mudrocks. *Fuel* 135, 359–373. doi:10.1016/j.fuel.2014.06.036

Li, T., Guo, H., Li, H., Lu, Y., and Xue, X. (2012). Research on Movable Fluids in Shale Gas Reservoirs with NMR Technology. *Spec. Oil Gas Reservoirs* 19 (1), 107–109+123. (in Chinese with English abstract).

Li, Y. (2021). Mechanics and Fracturing Techniques of Deep Shale from the Sichuan Basin, SW China. *Energ. Geosci.* 2 (1), 1–9. doi:10.1016/j.engeos.2020.06.002

Li, Y., Zhou, D. H., Wang, W. H., Jiang, T. X., and Xue, Z. J. (2020). Development of Unconventional Gas and Technologies Adopted in China. *Energ. Geosci.* 1 (1–2), 55–68. doi:10.1016/j.engeos.2020.04.004

Liu, X. (1995). Influence of clay Minerals on the Evolution of Organic Matter. *Nat. Gas Geosci.* 27 (6), 23–26. (in Chinese with English abstract).

Loucks, R. G., Reed, R. M., and Ruppel, S. C. (2009). Morphology, Genesis, and Distribution of Nanometer-Scale Pores in Siliceous Mudstones of the Mississippianbarnett Shale. *J. Sediment. Res.* 79 (11-12), 848–861. doi:10.2110/jsr.2009.092

Lu, J., Ruppel, S. C., and Rowe, H. D. (2015). Organic Matter Pores and Oil Generation in the Tuscaloosa marine Shale. *Bulletin* 99, 333–357. doi:10.1306/08201414055

Ma, Z., Zheng, L., Xu, X., Bao, F., and Yu, L. (2017). Thermal Simulation Experiments on the Formation and Evolution of Organic Pores in Organic-Rich Shale. *Acta Petrolei Sinica* 38 (1), 23–30. (in Chinese with English abstract).

Milliken, K. L., Rudnicki, M., Awwiller, D. N., and Zhang, T. (2013). Organic Matter-Hosted Pore System, Marcellus Formation (Devonian), Pennsylvania. *Bulletin* 97, 177–200. doi:10.1306/07231212048

Morozov, V. P., Jin, Z., Liang, X., Korolev, E. A., Liu, Q., Kolchugin, A. N., et al. (2021). Comparison of Source Rocks from the Lower Silurian Longmaxi Formation in the Yangzi Platform and the Upper Devonian Semiluksk Formation in East European Platform. *Energ. Geosci.* 2 (1), 63–72. doi:10.1016/j.engeos.2020.10.001

Nie, H., Jin, Z., and Zhang, J. (2018). Characteristics of Three Organic Matter Pore Types in the Wufeng-Longmaxi Shale of the Sichuan Basin, Southwest China. *Sci. Rep.* 8 (1), 7014. doi:10.1038/s41598-018-25104-5

Pommer, M., and Milliken, K. (2015). Pore Types and Pore-Size Distributions across thermal Maturity, Eagle Ford Formation, Southern Texas. *AAPG Bull.* 99 (9), 1713–1744. doi:10.1306/03051514151

Reed, R. M., Jobn, A., and Katberine, G. (2007). *Nanopores in the Mississippian Barnett Shale: Distribution, Morphology, and Possible Genesis: GSA Annual Meeting & Exposition*. Denver, Colorado, USADenver: The Geological Society of America, 1–6. October 28-31, 2007.

Santosh, M., and Feng, Z. Q. (2020). New Horizons in Energy Geoscience. *Energ. Geosci.* 1 (1–2), 1. doi:10.1016/j.engeos.2020.05.005

Slatt, R. M., and O'Brien, N. R. (2011). Pore Types in the Barnett and Woodford Gas Shales: Contribution to Understanding Gas Storage and Migration Pathways in fine-grained Rocks. *Bulletin* 95 (12), 2017–2030. doi:10.1306/03301110145

Sun, M., Yu, B., Hu, Q., Chen, S., Xia, W., and Ye, R. (2016). Nanoscale Pore Characteristics of the Lower Cambrian Niutitang Formation Shale: A Case Study from Well Yuke #1 in the Southeast of Chongqing, China. *Int. J. Coal Geology.* 154-155, 16–29. doi:10.1016/j.coal.2015.11.015

Tian, H., Zhang, S., Liu, S., Gao, Y., Zhang, H., Wang, M., et al. (2016). Evolution of Pores in Shale during thermal Maturation Using Small Angle X-ray Scattering (SAXS). *Pet. Geology. Exp.* 38 (1), 135–140. (in Chinese with English abstract).

Wang, G. (2020). Deformation of organic matter and its effect on pores in mud rocks. *Bulletin* 103, 21–36. doi:10.1306/04241918098

Wang, H., Shi, Z., Zhao, Q., Liu, D., Sun, S., Guo, W., Liang, F., Lin, C., and Wang, X. (2020). Stratigraphic framework of the Wufeng-Longmaxi shale in and Around the Sichuan Basin, China: Implications for Targeting Shale Gas. *Energ. Geosci.* 1 (3–4), 124–133. doi:10.1016/j.engeos.2020.05.006

Wang, P., Chen, Z., Jin, Z., Jiang, C., Sun, M., Guo, Y., et al. (2018). Shale Oil and Gas Resources in Organic Pores of the Devonian Duvernay Shale, Western Canada Sedimentary Basin Based on Petroleum System Modeling. *J. Nat. Gas Sci. Eng.* 50, 33–42. doi:10.1016/j.jngse.2017.10.027

Wu, J., Liu, D., and Yao, Y. (2014). Characteristics and Controlling Factors of Nanopores in Shales in Weibei, Ordos Basin. *Oil Gas Geology.* 35 (4), 542–550. (in Chinese with English abstract).

Wu, S., Zhu, R., Cui, J., Cui, J., Bai, B., Zhang, X., et al. (2015). P Characteristics of Lacustrine Shale Porosity Evolution, Triassic Chang 7 Member, Ordos Basin, NW China. *Pet. Exploration Develop.* 42 (2), 167–176. (in Chinese with English abstract). doi:10.1016/s1876-3804(15)30005-7

Wu, T., Li, L., Li, W., Gai, Y., Qiu, J., Pan, G., et al. (2021). A Quantitative Study on Source Rocks in the Western Leidong Depression, Northern South China Sea. *Energ. Geosci.* 2 (1), 73–82. doi:10.1016/j.engeos.2020.10.002

Yang, F., Ning, Z., and Kong, D. (2013). Analysis of Shale Pore Structure by High-Pressure Mercury Intrusion Method and Nitrogen Adsorption Method. *Nat. Gas Geosci.* 24 (3), 450–455. (in Chinese with English abstract).

Yao, J., and Zhao, X. (2010). *Digital Core and Pore Level Seepage Simulation Theory*. Beijing: Petroleum Industry Press, 125–128.

Yu, B. (2013). Classification and Characterization of Gas Shale Pore System. *Earth Sci. Frontier* 20 (4), 211–220. (in Chinese with English abstract).

Zhang, J., Jin, Z., and Yuan, M. (2004). Reservoiring Mechanism of Shale Gasand its Distribution. *Nat. Gas Industry* 24 (7), 15–18. (in Chinese with English abstract).

Zhang, J., and Zhang, P. (1996). Discussion on the Catalytic Effect of Pyrite on Organic Hydrocarbon Formation. *Adv. Earth Sci.* 11 (3), 282–287. (in Chinese with English abstract).

Zhang, Q., Zhu, X., Li, C., Qiao, L., Liu, C., Mei, X., et al. (2016). Classification and Quantitative Characterization of Microscopic Pores in Organic-Rich Shale of the Shahejie Formation in the Zhanhua Sag, Bohai Bay Basin. *Oil Gas Geology.* 37 (3), 422–432+438.

Zhao, Z., Wu, K., Fan, Y., Guo, J., Zeng, B., and Yue, W. (2020). An Optimization Model for Conductivity of Hydraulic Fracture Networks in the Longmaxi Shale, Sichuan basin, Southwest China. *Energ. Geosci.* 1 (1–2), 47–54. doi:10.1016/j.engeos.2020.05.001

Zou, C., Dong, D., Wang, S., Li, J., Li, X., Wang, Y., et al. (2010). Geological Characteristics and Resource Potential of Shale Gas in China. *Pet. Exploration Develop.* 37 (6), 641–653. (in Chinese with English abstract). doi:10.1016/s1876-3804(11)60001-3

Zou, C., Dong, D., and Yang, H. (2011). Formation Conditions and Exploration Practice of Shale Gas in China. *Nat. Gas Industry* 31 (12), 26–39. (in Chinese with English abstract).

Zou, C., Zhu, R., Bai, B., Yang, Z., Wu, S., Su, L., et al. (2011). First Discovery of Nano-Pore Throat in Oil and Gas Reservoir in China and its Scientific Value. *Acta Petrologica Sinica* 27 (6), 1857–1864. (in Chinese with English abstract).